Digital Simulation and Recreation of a Vacuum Tube Guitar Amp

by

John Ragland

A thesis submitted to the Graduate Faculty of
Auburn University
in partial fulfillment of the
requirements for the Degree of
Master of Science

Auburn, Alabama
May 2, 2020

Keywords: guitar, amplifier, nonlinear modeling, digital audio, vacuum-tube, distortion, signal processing, real-time simulation, guitar effects pedal

Approved by

Thaddeus Roppel, Associate Professor, Electrical and Computer Engineering
Christopher Harris, Assistant Professor, Electrical and Computer Engineering
Yin Sun, Assistant Professor, Electrical and Computer Engineering

Abstract

This thesis presents the process of designing, building, and testing a system that will be referred to herein as the Digital Guitar Amplifier. The Digital Guitar Amplifier is a real time digital audio signal processing unit that implements a signal processing algorithm that emulates the sound of a Fender Blues Jr. The Digital Guitar Amplifier fits within a reasonable footprint for a guitar effects pedal. The digital signal processor has CD level audio quality. The signal processing algorithm attempts to maintain the legacy of the vacuum tube within the math and processing of the algorithm by physically modelling the vacuum tube circuit. A mathematical comparison and human hearing survey is presented, which demonstrates that the sound of the Digital Guitar Amplifier compares favorably to the sound of a real Fender Blues Jr. amplifier. The algorithm that is developed can be extended to emulate any tube amplifier.

Acknowledgments

I would like to thank my advisor Dr. Roppel for his guidance throughout my thesis research and writing process. I would like to thank Dr. Harris and Dr. Sun for being my masters thesis committee members. I would like to thank John Tennant and Michael Eddy for helping with soldering the designed circuit board. I would like to thank all of the participants in the hearing survey. Lastly, I am grateful for my wife, Madison Ragland, for her encouragement and making it possible to pay the bills.

Table of Contents

List of Tables

List of Figures

List of Abbreviations

DAWs	Digital Audio Workstations
VTGAA	Vacuum Tube Guitar Amp Algorithm
IIR	Infinite Impulse Response
LTI	Linear Time Invariant
SNR	Signal to Noise Ratio
FT	Fourier Transform

I. Introduction

In the early 1950s, blues guitarists started experimenting with a previously undesirable effect from their low fidelity vacuum tube guitar amplifiers. If they drove their amplifiers beyond the designed capabilities, the sounds that would be produced had a unique, fuzzy tone. This was the birth of overdrive or distortion. These blues guitarists began using this phenomenon as a tool to be more expressive with their music. The unique sound exploded in popularity and has come to define popular music ever since.

As vacuum tubes became increasingly replaced by the cheaper, more reliable transistors, it was soon discovered that the distortion created by transistors was less audibly desirable than that of their vacuum tube predecessors. The harmonics that are added to a signal from vacuum tube distortion are different from the harmonics added to a signal by transistors. Whether or not vacuum tube distortion is innately more pleasing to the human ear or is simply due to the nostalgic sounds of the musical eras of the 1960s and 1970s, some guitarists have opted to still use vacuum tube amplifiers instead of transistor amplifiers.

Even though vacuum tube amplifiers produce more preferable tonal qualities for some people, they do have considerable drawbacks. They are more expensive to produce and replacement parts are becoming more expensive as production of vacuum tubes decreases. Additionally, since vacuum tube amplifiers require an audio transformer and vacuum tube mounting hardware, they are considerably heavier than transistor amplifiers. Considering these problems, it is advantageous to have a system that can create the desired tonal qualities of a vacuum tube amplifier without actually having to use the physical devices. In this thesis, I create a digital audio processing algorithm that physically simulates the electrical characteristics of a Fender Blues Jr. guitar amplifier, while attempting to maintain the physical legacy of this

specific amplifier design. Additionally, this algorithm is implemented in a custom built digital audio processing system that can fit inside of a guitar effects pedal. Lastly, the built system is mathematically and audibly compared to the original Fender Blues Jr. guitar amplifier.

II. Literature Review

Ever since transistors started replacing vacuum tubes as a cheaper and lower power alternative for audio amplification, there have been claims that the ‘warm’ sound of a vacuum tube is unmatched. Papers such as [1] and [2] explore the mathematical differences between transistors and vacuum tubes. [2] states that when a tube amplifier is operated in the linear region it is indistinguishable from its solid state counter parts. One starts to see major mathematical differences in the behaviors of the two systems when the circuits are overdriven.

Looking at clipped waveforms on an oscilloscope starts to reveal some of the differences present between vacuum tube clipping and transistor clipping. Figure 1(left) shows the measured output of the second stage of the pre-amplifier from the Fender Blues Jr. guitar amplifier. Figure 1(right) shows the SPICE simulation of a clipped CE transistor amplifier.

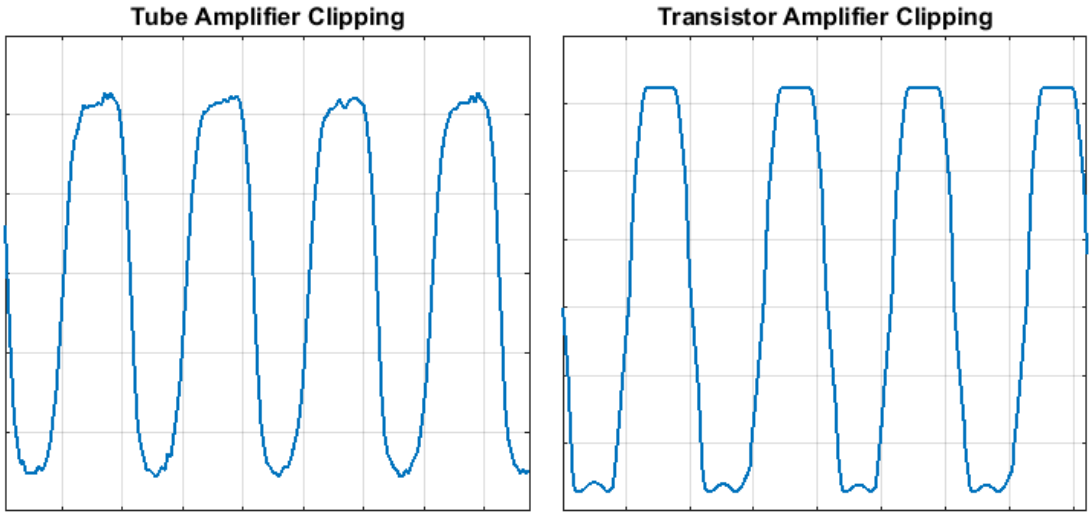

Figure 1: Vacuum Tube Clipping Compared to Transistor Clipping

It can be seen that the vacuum tube clips in a much rounder fashion. The sharp edges of the transistor clipping create different higher frequency harmonic components as compared to the rounder clipping of the vacuum tube.

Since the tonal qualities of the vacuum tube amplifiers are unique and desired by many guitar players, it is advantageous to attempt to design digital recreations of the sound of vacuum tube amplifiers. This would allow for more robust systems that could replicate a multitude of vacuum tube amplifiers designs simply by uploading a new designed algorithm. Many commercially available digital audio workstations (DAWs) have built in plugins that allow a user to plug their instrument directly into the computer audio interface and add audio effects after the fact or in real time. As is the case for almost all audio applications, the algorithms that these professional software packages use are proprietary and highly competitive. Below is a brief overview of some of the developments in digitally modelling vacuum tube audio amplifiers over the years. Since the development of these tube emulation techniques is commercially viable, most of the references are patents.

An early technique to digitally model guitar distortion was static waveshaping with memoryless nonlinearities. This technique creates a nonlinear mapping from the input voltage to the output voltage and is illustrated in Figure 2. Figure 2 demonstrates a simple clipping device in which any amplitude over 1 is clipped to 1. In a patent filed by Yamaha [3], the nonlinear mapping chosen to emulate the sound of a tube is given by (1)

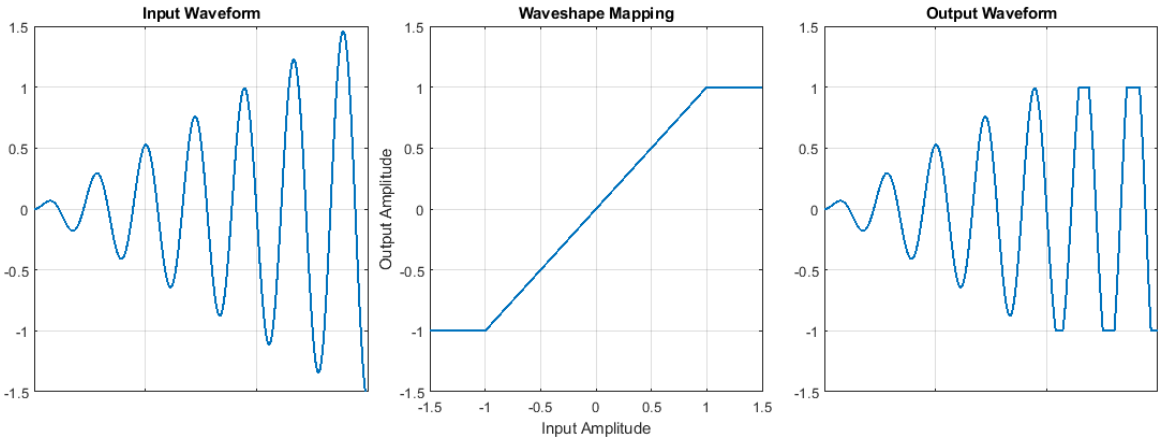

Figure 2: Demonstration of Waveshaping

$$y = \frac{3x}{2}\left(1 - \frac{x^2}{3}\right) \quad (1)$$

There have been other attempts to improve upon the waveshaping technique, including different functional mappings than (1) and also mappings defined by lookup tables to more closely match the tube amplifier response. Some of these patents include[4] [5].

The main problem with the waveshaping technique is that it is a memoryless nonlinear algorithm. In the physical vacuum tube amplifier, both designed capacitors and parasitic capacitances are present. These capacitors add memory to the amplifier system. One solution to this is dynamic waveshapers. These designs change their input to output mapping depending on the input signal or calculated system states. An example of a system using this technique is outlined in [6].

These techniques can produce decent results, but they do not physically model the vacuum tube. Instead, they attempt to replicate the audio effects of a vacuum tube with little consideration given to the physical phenomena that are occurring in an actual vacuum tube amplifier. The method outlined in [7] and [8] uses a SPICE model of a pre-amplifier stage of a vacuum tube amplifier simulated in real time. This method can retain the physical phenomena of the vacuum tube amplifier. In theory, if the SPICE model of the tube amplifier is a perfect representation of a vacuum tube, this method would almost perfectly recreate the response of a tube pre-amplifier stage. There would only be nominal error created from look up table interpolation required to run the algorithm in real time. This method is the basis for what is used in the algorithm design within this thesis.

III. Methodology

The hardware and software used to design and build the Digital Guitar Amplifier is listed below. All computer programming used to design the algorithm was accomplished with MATLAB r2019b. The computer used to run the simulations was an HP Compaq 8200 desktop computer with an Intel i7 core processor with 8GB of RAM. The Teensy 4.0 microcontroller was used as the microcontroller for the real time audio processing unit. The Teensy 4.0 was programmed using the Arduino IDE. LTspice XVII was used for circuit simulations. The schematic and PCB were created using KICAD version 5.1.2. The PCB printing service PCBWAY was used to print the circuit board. All circuit board elements were hand soldered with help from the Auburn Electrical Engineering Department Shop. All data from the Fender Blues Jr. guitar amplifier was acquired using a Tektronixs TDS7104 Digital Phosphor Oscilloscope. The human hearing survey was conducted using Qualtrix. The stereo microphones used to record the audio were the Samson CO2 Stereo Pair. The audio was recorded at 24 bit resolution, sampled at 44.1 kHz. The computer audio interface used to record the audio was the Presonus AudioBox USB. The PA speaker that was used to amplify the Digital Guitar Amp was a Harbinger APS12 active powered speaker.

IV. Algorithm Design

The vacuum tube guitar amplifier algorithm (VTGAA) was designed by attempting to physically model the circuit components of the Fender Blues Jr. guitar amplifier. The full schematic for the Fender Blues Jr. is available online [9] and is also included in appendix I. The Fender Blues Jr. can be divided into three separate sub systems: the pre-amplifier stage and tone-stack, the reverb stage, and the power amplifier stage.

The pre-amplifier stage consists of three triode amplifier stages that are built in the common cathode configuration using 12AX7 vacuum tubes. These stages provide adequate buffering for the guitar signal. Electric guitars generate their electric signals through magnetic coils. They subsequently have very low voltage and power levels and therefore, require very high input impedances for the amplifier. The pre-amplifier stage also has a gain of approximately 420 $^{v}/_{v}$ (determined from test levels cited in [9]). The tone stack is between the second and third pre-amplifier stage. The tone stack is a third order RC filter that can be modulated by the user by changing the position of potentiometers. This circuit provides the bass, middle, and treble controls to the guitar user. The pre-amplifier stage also has a volume control which controls the input voltage to the second stage of the pre-amplifier.

The reverb stage uses a spring reverb. Spring reverb was originally developed as a cheap simulation of echo in a room by Hammond Laurens [10] for his electric organs. This system works by using magnets to vibrate a mechanical spring. At the other end of the spring, the vibrations are converted back into an electrical signal. This ‘wet’ signal is then mixed back with the original ‘dry’ waveform to produce variable reverberation. Since the invention of the spring reverb, better techniques have been developed to emulate the echo of a room, but since the spring

reverb has such a unique sound, it is usually tied to specific eras of music and has become a sought after audio effect in and of itself.

The output of the spring reverberation stage is then put into the power amplifier stage. The input voltage level to the power amplifier stage is controlled by the master control knob, which acts as a voltage divider. This stage consists of 2 12AX7 vacuum tubes and 2 6805 vacuum tubes and makes the audio signal powerful enough to drive a loudspeaker. The signal is then put through an audio transformer to impedance match to the loudspeaker.

There are nonlinearities that are added at every subsystem of the Fender Blues Jr. amplifier. In normal operation, the power amplifier should not clip. However, small signal distortion can still effect the guitar audio. Additionally, the audio transformer can add nonlinearities through the effect of hysteresis. The spring reverberation system is nonlinear by nature. The hypothesis presented in this thesis however is that the ‘vacuum tube tone’ that guitar players seek is almost completely created by clipping in the second stage of the preamplifier subsystem and the tone stack. This assumption is made because the volume knob on the Fender Blues Jr. solely controls the input amplitude to the second stage of the preamplifier subsystem. Therefore, the aspect of the vacuum tube guitar amplifier that will be nonlinearly, physically modelled is the second stage of the pre-amplifier subsystem. The tone stack will also be physically modelled, however it is linear in nature and can be implemented with a infinite impulse response (IIR) digital filter. In subsequent sections, I will outline, sequentially, the aspects of the designed VTGAA. A demo of the VTGAA can be found at https://github.com/John-Ragland/Thesis.

A. Physically Modelling Pre-Amplifier Second Stage

In the Fender Blues Jr. Guitar Amplifier, distortion can be achieved by turning the volume knob up all the way and turning the main knob down to around 2 or 3. The volume knob controls the input voltage to the second stage of the pre-amplifier. The master knob controls the input voltage of the power amplifier. From this information, it can be determined that most of the guitar signal clipping is happening in the second stage of the pre-amp. Figure 3 shows the schematic of the common cathode tube amplifier used in the Fender Blues Jr. This is the circuit that was physically modelled in real time. The transistor at the bottom functions to short out the resistor R9 when the 'fat switch' is selected. This results in a louder, richer tone. The algorithm was created assuming the resistor was shorted out, however it would be easy to add a 'fat switch' capability in the future by being able to switch between separate circuit simulations.

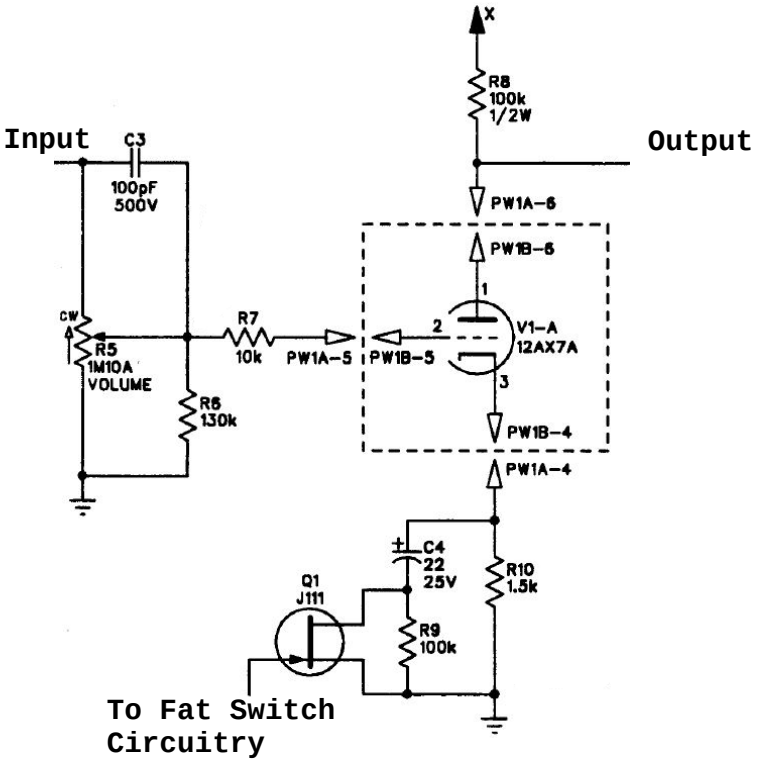

Figure 3: Second Stage of Fender Blues Jr. Preamplifier Subsystem

1) Differential Equations

The technique used to model the characteristics of the pre-amp is based on [7] and [8] and is outlined below. For any nonlinear circuit, a set of ODE's of the form

$$\dot{\mathbf{x}} = \mathbf{Ax} + \mathbf{Bu} + \mathbf{Ci} \tag{2}$$

$$\mathbf{i} = \mathbf{f}(\mathbf{v}) \tag{3}$$

$$\mathbf{v} = \mathbf{Dx} + \mathbf{Eu} + \mathbf{Fi} \tag{4}$$

can be derived. Where $\boldsymbol{x}$ are the state variables of the system, $\boldsymbol{u}$ are the system inputs and $\boldsymbol{i}$ are the system nonlinearities. For this circuit, $\boldsymbol{x}$ was chosen to be the voltages across every capacitor, $\boldsymbol{u}$ was chosen to be all signal sources and DC voltage sources, and $\boldsymbol{i}$ was chosen to be grid and plate currents. The Koren Model [11] of the Vacuum Tube amplifier was used which gives **f** to be (5)

$$\boldsymbol{f} = \begin{bmatrix} \mathrm{I_g}(\mathrm{V_{gk}}, \mathrm{V_{pk}}) = \log\left(1 + \exp\left(\frac{V_{gk}}{V_T}\right)\right)\frac{V_T}{R_G} \\ I_p(V_{gk}, V_{pk}) = \frac{E_d^{Kx}}{K_{G1}}\left(1 + sign(E_d)\right) \end{bmatrix} \tag{5}$$

where

$$E_d = \frac{V_{pk}}{K_p}\log\left(1 + \exp\left(K_p\left(\frac{1}{\mu} + \frac{V_{gk}}{\sqrt{K_{VB} + V_{pk}^2}}\right)\right)\right)$$

Matrices **L**, **M**, and **N** can then be derived to give an expression for the output given the state, input, and nonlinearities of the circuit (6). In general, y can be a vector up to length n such that $\boldsymbol{x} \in \mathbb{R}^n$. However for this circuit, only one output is needed.

$$\mathrm{y} = \mathbf{Lx} + \mathbf{Mu} + \mathbf{Ni} \tag{6}$$

Using numerical methods, (2) (3) and (4) can be discretized and a state update equation can be derived in discrete time.

2) Discretizing Solution Using Backward Euler

The ordinary differential equations are discretized using the Backward Euler method [12, p. 57]**.** The equation for Backward Euler is given in (7)

$$\dot{\boldsymbol{x}}[n] = \alpha(\boldsymbol{x}[n] - x[\boldsymbol{n} - 1]) \tag{7}$$

where $\alpha = F_S$, and F_s is the sampling frequency of the digital signal processing system. Plugging (7) into (2) gives the state update equation (8).

$$\boldsymbol{x}[n] = \alpha \boldsymbol{H}\boldsymbol{x}[n-1] + \boldsymbol{H}(\boldsymbol{B}\boldsymbol{u}[n] + \boldsymbol{C}\boldsymbol{i}[n]) \tag{8}$$

where

$$\boldsymbol{H} = (\alpha \boldsymbol{I} - \boldsymbol{A})^{-1}$$

Then, plugging (8) and (3) into (4), one can solve for the updated voltage values using the previous state and the input values. However, (4) is nonlinear and implicitly defined and must be solved using iterative methods. The trust-region dogleg algorithm [13] is an iterative nonlinear implicit equation solving algorithm that guarantees convergence. This algorithm is the default function solving algorithm used in the MATLAB function fsolve(). However, this algorithm is computationally heavy and is not realizable in real time. In order to solve this problem, a lookup table containing a reasonable set of nonlinear values must be precomputed to allow for real time simulation.

3) Device Nonlinearity Derivation

First, let's plug (4) into (3) to get (9).

$$\mathbf{i}[\mathrm{n}] = \mathbf{f}(\mathbf{D}\mathbf{x}[\mathrm{n}] + \mathbf{E}\mathbf{u}[\mathrm{n}] + \mathbf{F}\mathbf{i}[\mathbf{n}]) \tag{9}$$

Now, (8) is plugged into (9) to yield (10).

$$\mathbf{i}[\mathrm{n}] = \mathbf{f}\begin{pmatrix}\alpha\mathbf{DHx}[\mathrm{n}-1] + (\mathbf{DHB}+\mathbf{E})\mathbf{u}[\mathrm{n}] \\ +(\mathbf{DHC}+\mathbf{F})\mathbf{i}[\mathrm{n}]\end{pmatrix} \tag{10}$$

If one defines **K** (constant) and **P** (parameter) as

$$\mathbf{K} = \mathbf{DHC} + \mathbf{F} \tag{11}$$

$$\mathbf{p}[\mathrm{n}] = \alpha\mathbf{DHx}[\mathrm{n}-1] + (\mathbf{DHB}+\mathbf{E})\mathbf{u}[\mathrm{n}] \tag{12}$$

then (10) can be rewritten as (13), which is an implicit equation for **i**[n] with one parameter, **p**[n].

$$\mathbf{0} = \boldsymbol{f}(\boldsymbol{p}[n] + \boldsymbol{K}\boldsymbol{i}[n]) - \boldsymbol{i}[n] \tag{13}$$

For the case of the vacuum tube pre amp stage, (13) is functional and can be represented as a nonlinear mapping (14), which was computed offline using MATLAB's implicit solvers and a lookup table was created. The lookup table was designed to be size 100 by 100 and span all reasonable input values.

$$\boldsymbol{i}[n] = \mathbf{g}(\mathbf{p}[\mathrm{n}]) \tag{14}$$

Figure 4 and Figure 5 show the lookup tables for the range of possible **p**[n] values.

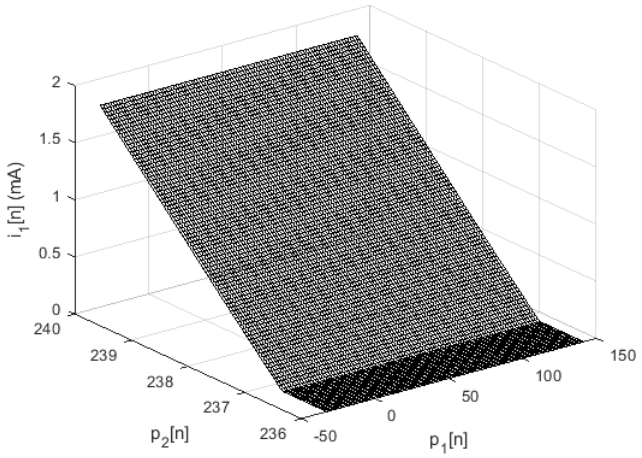

Figure 4: Plot of $\mathbf{g_1(V)}$ Lookup Table for $\mathbf{i_1}$

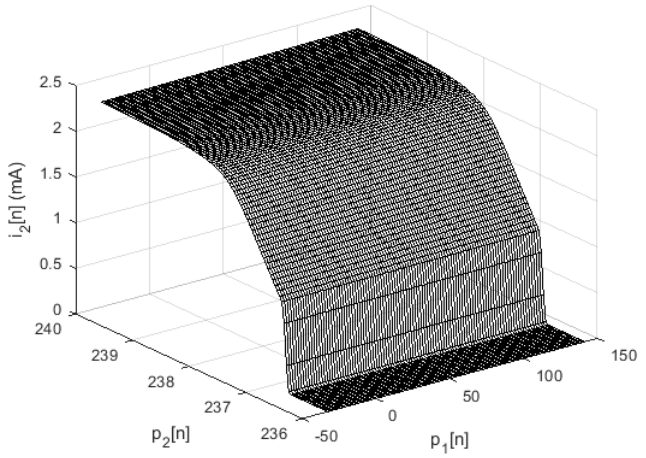

Figure 5: Plot of $\mathbf{g_1}(\mathbf{V})$ Lookup Table for $\mathbf{i_2}$

4) State Update Procedure.

The derivations above give way to the state update procedure outlined below, which can be used as a real time audio processing algorithm [7, p. 730].

1. Compute **p**[n] using (12).
2. Compute **i**[n] using lookup tables and bilinear interpolation.
3. Calculate state update using (8).
4. Compute outputs using (6)

This results in the vast majority of computations required to simulate the circuit to be computed offline using MATLAB. The real time digital signal processor must simply calculate the state update and then calculate the output for each measured input.

B. EQ System

The Fender Blues Junior amplifier, and many other amplifiers from the era, has an EQ filter that will, from here on, be referred to as the tone stack. This filter consists of resistors, capacitors, and potentiometers, and is a 3rd order, passive filter. The method used to discretize this filter for digital recreation is described in [14]. The circuit of the filter is shown in Figure 6.

The potentiometers are modeled as two resistors. The position of the potentiometer knob is indicated by the variables mid, low or treb (ranging in value from 0 to 1). Unmarked units for capacitance are assumed to be μF.

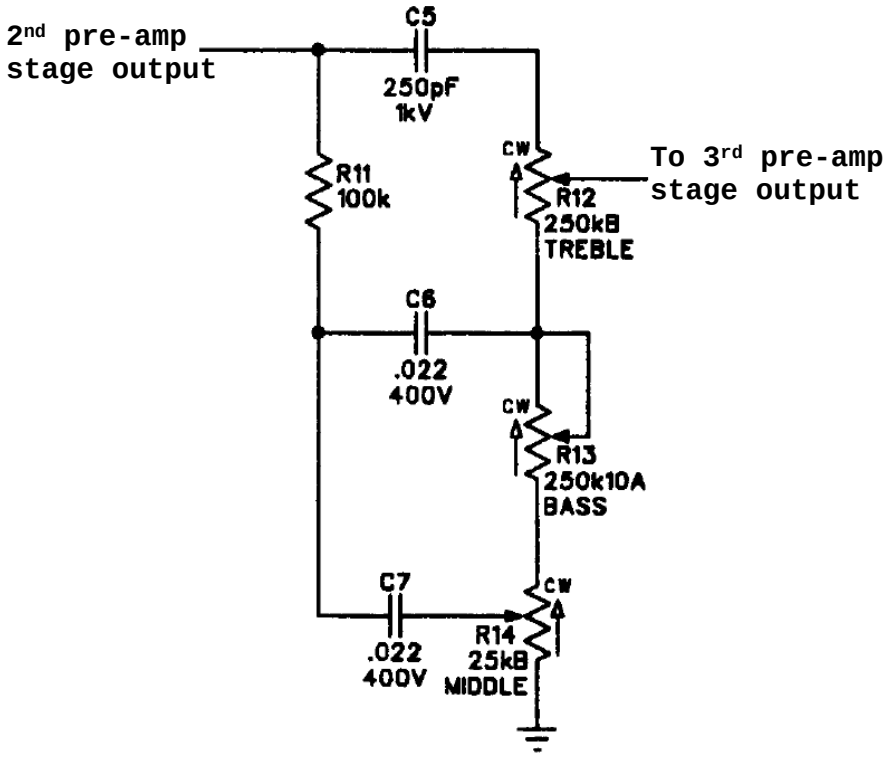

Figure 6: Schematic of Tone Stack in Fender Blues Jr. Amplifier

First, an analytical expression for the transfer function in the s domain was computed using circuit analysis techniques. This results in a transfer function of the form (15), where the coefficients are functions of $mid, bass,$ and $treb$ [14, p. 1].

$$H(s) = \frac{b_1 s + b_2 s^2 + b_3 s^3}{a_0 + a_1 s + a_2 s^2 + a_3 s^3} \tag{15}$$

The bilinear transform of (15) was found using the substitution (16). This resulted in H(z), which has the form (17), where the coefficients are functions of $mid, low,$ and $treb$. These functions were found using MATLAB's Symbolic Toolbox to be (18) and (19). m, l and t were used in

place of mid, low, and $treb$ for brevity. These coefficients can be calculated in real time and updated every time that the microcontroller reads the values of the potentiometers.

$$s = \frac{2}{T} \cdot \frac{1 - z^{-1}}{1 + z^{-1}} \tag{16}$$

$$H(z) = \frac{B_0 + B_1 z^{-1} + B_2 z^{-2} + B_3 z^{-3}}{A_0 + A_1 z^{-1} + A_2 z^{-2} + A_3 z^{-3}} \tag{17}$$

$$\begin{aligned}
B_0 &= 51888.5mt - 20856.9m - 54033.3t - 205409lm - 518885.0lt - 5304.02l \\
&\quad + 20540.9m^2 - 530.402, \\
B_1 &= 4322.79l + 57081.8m + 157799.0t + 568629.0lm + 1556666.0lt - 155666.0mt \\
&\quad - 56862.9m^2 + 432.279, \\
B_2 &= 5304.02l - 51787.0m - 153521.0t - 521030.0lm - 1556666.0lt + 155666.0mt \\
&\quad + 52103.0m^2 + 530.402, \\
B_3 &= 15562.1m - 4322.79l + 49754.7t + 157810.0lm + 518885.0lt - 51888.5mt \\
&\quad - 15781.0m^2 - 432.279
\end{aligned} \tag{18}$$

$$\begin{aligned}
A_0 &= 40444.5m - 618318.0l - 205409.0lm + 20540.9m^2 - 64365.7, \\
A_1 &= 1655111.0l - 107997.0m + 568629.0lm - 56862.9m^2 + 167253.0, \\
A_2 &= 94465.6m - 1457222.0l - 521030.0lm + 52103.0m^2 - 143192.0, \\
A_3 &= 420433.0l - 26913.5m + 157810.0lm - 15781.0m^2 + 40296.6
\end{aligned} \tag{19}$$

V. High Fidelity, Real Time Digital Audio Processing Unit

When an electric guitar is plugged directly into a sound system, the EQ will usually sound wrong and there will also be no access to the guitar distortion effects that are created using an amplifier designed specifically for a guitar. Currently, products exist that allow the user to use plugins from their computer to create audio effects. This is cumbersome because you need a computer running specific software for a live performance. It would therefore be advantageous to have a guitar effects pedal like device that is capable of implementing the algorithm that was designed for this thesis. Therefore, another goal of this thesis was to build a digital audio processor that had CD level audio quality that could fit inside of a reasonable guitar effects pedal footprint. Therefore, if a guitar player needed to plug directly into a sound system, they could use this as a way to condition their sound to make it sound as if they are actually plugged into a guitar amplifier instead of a sound system.

The processor that was chosen for this project was the Teensy 4.0 by PJRC [15]. It is far faster than its competitors and therefore allows for the computations required to implement the VTGAA. Figure 7 shows the block diagram of the system, and the schematic used to print the circuit board is in Appendix 2. Below, each section of the circuit is described in detail.

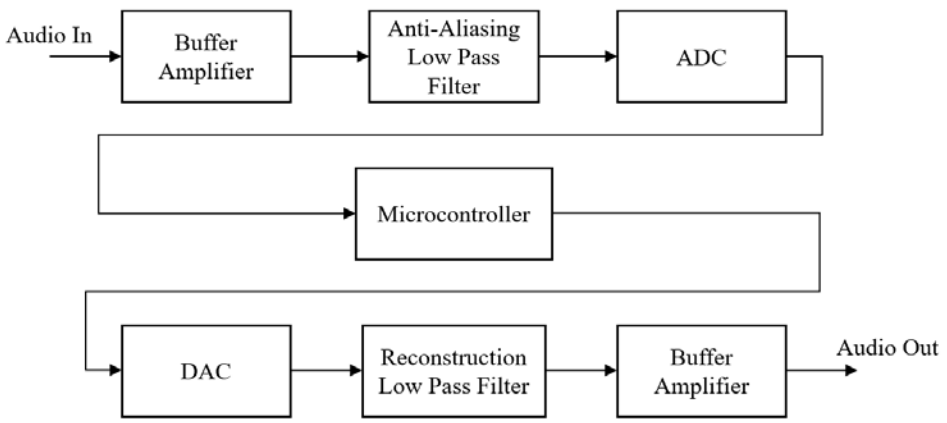

Figure 7: Block Diagram of the Audio Processing Unit

A. Input Buffer Amplifier

For the input buffer amplifier block of the audio processing unit, an op-amp configuration of a unity gain amplifier and an inverting amplifier configuration were connected in series. The purpose of this section is to provide a high input impedance to the input port, which is connected to the electric guitar. The analog signal from the electric guitar has very low power, requiring the buffer amplifier stage. Additionally, the amplitude of the signal from the electric guitar is low compared to the dynamic range of the ADC. Therefore, an amplifier must be designed to amplify the input signal so that the dynamic range of the ADC is fully utilized. Lastly, a DC bias must be introduced to the signal because the ADC is powered by a single ended supply. The DC bias was accomplished by powering the buffer amplifier stage from a single ended supply as well. The maximum output amplitude for a Fender Stratocaster, which uses single coil electric guitar pickups, was measured to be approximately 552 mV peak to peak. Another common electric guitar pickup style is the humbucker. The maximum output amplitude for an Epiphone Joe Pass Emperor II, which uses the humbucker pickup, was measured to be approximately 856 mV peak to peak. These voltage values and regularly available resistor values were used to design the

inverting amplifier to have a gain of $A_v = 6.8\frac{v}{v}$. The dynamic range of the ADC is 5V. This gain value results in guitars using humbucker pickups to clip slightly. This can be solved by the user turning the volume knob down on the guitar. The higher gain, however, allows for a larger resolution for guitars using single coil pickups. Figure 8 shows the schematic of the buffer amplifier stage of the audio processing unit. The op-amp used in this circuit was the OPA2313 [16].

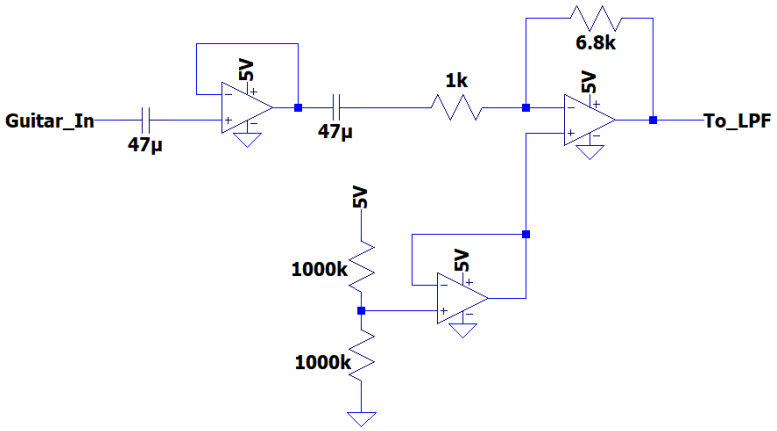

Figure 8: Schematic of Input Amplifier

B. Anti-aliasing Low Pass Filter

The circuit was designed to sample the signal at 44.1 kHz using 16 bits per sample. This, relatively high sample and bit rate is the same as CD quality audio, which was designed around the capabilities of the human hearing system. If a time signal is sampled at 44.1 kHz, then the largest frequency component that can be captured is 22.05 kHz. An anti-aliasing filter was chosen to have a cutoff frequency of 20 kHz. The specific low pass filter that was chosen was the LTC1069-6 Single Supply, Very Low Power, Elliptic Lowpass filter [17]. This is an eighth order, switched capacitor, low pass filter. The cutoff frequency is set to 1/50th of the clock frequency with a maximum cutoff of 20 kHz. This filter samples twice a clock cycle, and

attenuates up to the Nyquist rate, which is 1 MHz for this project. This clock signal was generated from the Teensy 4.0. Any frequency above 1MHz is not attenuated, but is far above the audible range. One issue that will be discussed further in the results section is that there is an audible noise that is added to the output of this lowpass filter.

C. Analog to Digital Converter

The analog to digital converter that was chosen for this project is the Maxim Integrated MAX11100 [18]. This ADC has 16-bit resolution. The ADC has separate power for the digital and analog functions. The analog power supply was set to 5 V. The digital power supply was set to the voltage level of the Teensy 4.0, which is 3.3V. The ADC communicates with the microcontroller over a SPI interface operating at 4.7 MHz. The ADC requires an external voltage reference which is supplied by the MAX6029 [19] which provides a voltage reference of 4.1 V.

D. Teensy 4.0 Microcontroller

The Teensy 4.0 microcontroller, created by PJRC [15], was selected as the processor for this project because of its power and small footprint. The Teensy 4.0 was programmed using the Arduino IDE, and the code used to program it is available at https://github.com/John-Ragland/Thesis.

E. Digital to Analog Converter

The digital to analog converter used for this circuit was the LTC1655 [20]. The DAC has 16-bit resolution, and was powered by a single ended 3.3 V supply. It is interfaced with the Teensy 4.0 microcontroller using a SPI interface operating at 10 MHz.

F. Reconstruction Filter

The reconstruction filter was designed to have the same cutoff frequency as the anti-aliasing filter. The filter used was the LTC1069-6 Single Supply, Very Low Power, Elliptic

Lowpass filter [17]. This filter is identical to the anti-aliasing filter, and the same clock signal was used for both.

G. Output Buffer Amplifier

The output buffer amplifier took the 3.3 V peak to peak output of the digital to analog converter and converted it to the audio line level voltage value of 1 V peak to peak. The DC component was also removed with a $47\mu F$ capacitor in series. The designed gain was $\mathrm{A}_v = 0.3\ {}^{v}/_{v}$.

VI. Results

To evaluate the effectiveness of the Digital Guitar Amp, the following methods were used and are outlined below. The algorithm to physically model the second stage of the pre-amplifier of the Fender Blues Jr. was compared to the actual output of the Fender Blue Jr. output visually and audibly. The algorithm that was implemented with lookup tables was compared to an iteratively solved simulation. The designed digital filter to simulate the tone stack response was compared to the continuous time response of the tone stack by looking at squared error vs. frequency. Lastly, a human hearing survey was conducted to compare the audible differences between the Fender Blues Jr. and the Digital Guitar Amp.

A. Algorithm to Physically Model Second Stage of Pre-Amplifier

Figure 9 (left) shows the output of the second stage of the Fender Blues Jr. and the output of the simulated output using the VTGAA. Figure 9 (right) shows the spectrum of the Fender Blues Jr. and the output of the simulated output using the VTGAA. The same input was used for both. As is shown in Figure 9, the simulation does not work perfectly. Most notably, the actual tube amplifier saturates at an output voltage lower than the voltage supply, which is 238 volts. The simulation saturates fairly sharply at the 238 volt mark. As is described above, this error is not introduced from the lookup table. Therefore, my theory as to where this discrepancy originates from is the SPICE model of the vacuum tube [11]. Designing a better, and more accurate SPICE model for the 12AX7 vacuum tube could solve this issue, but is beyond the scope of this thesis.

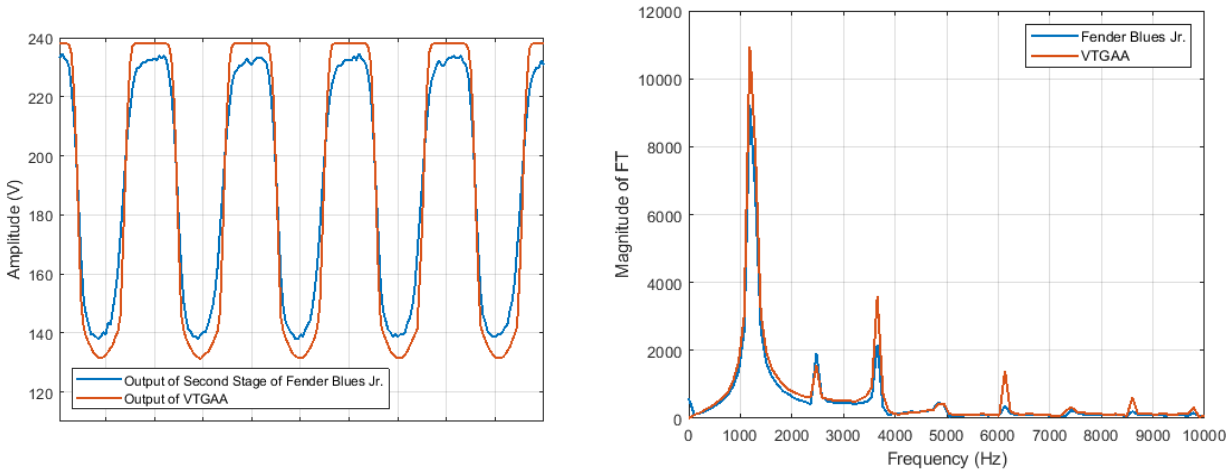

Figure 9: Comparison of VTGAA Simulated Output to Actual Fender Blues Jr. Output

Figure 10 shows a comparison of the VTGAA and the actual Fender Blues Jr. when operating in the linear region of the vacuum tube. As is shown, the simulation follows the actual output fairly nicely. The larger discrepancies are only prevalent when the system is oversaturated.

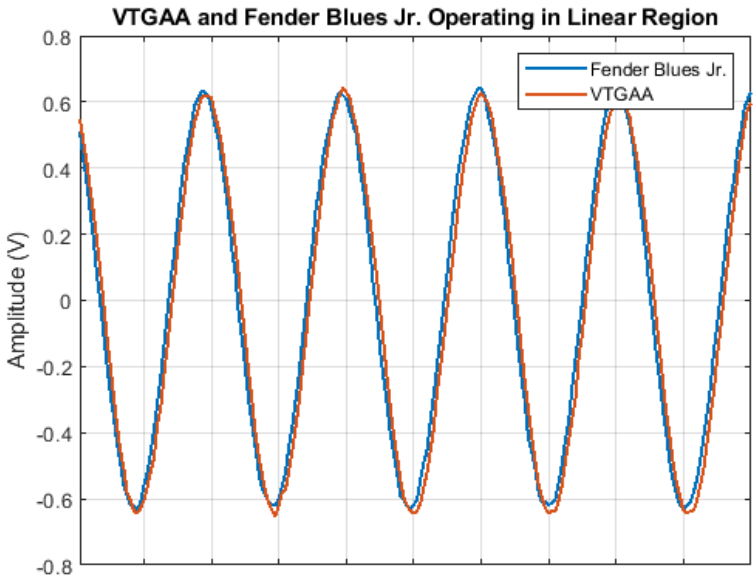

Figure 10: Comparison of Fender Blues Jr. and VTGAA Operating in Linear Region

For the sake of this simulation, numerical errors are assumed to be negligible. All simulations were conducted as outlined in the methodology chapter. Therefore, all numerical calculations had 16 digits of precision. Additionally, any errors from the numerical methods used to solve the implicitly defined, nonlinear equation outlined in section IV.3 are also assumed to be negligible. In order to run the VTGAA in real time, however, a look up table for this implicit nonlinear function had to be computed. This error was not negligible and changed the shape of the waveform slightly. Figure 11 shows the simulated output using the nonlinear, implicit, equation solver described in section IV. Figure 12 shows the simulated output using a precomputed lookup table. Figure 13 shows the simulation output using the lookup table and then using bilinear interpolation. Figure 14 shows a comparison in the time domain of the simulation using the nonlinear, iterative, solver and the simulation using a lookup table and bilinear interpolation. Figure 15 shows the error of the signals in Figure 11 and Figure 13 as a percent of the voltage range of the output. Figure 16 shows a comparison of the spectrum of the two signals in Figure 11 and Figure 13. As is shown, the act of using a lookup table suppresses the small even harmonics that are present in the simulation that uses the nonlinear, iterative, solver.

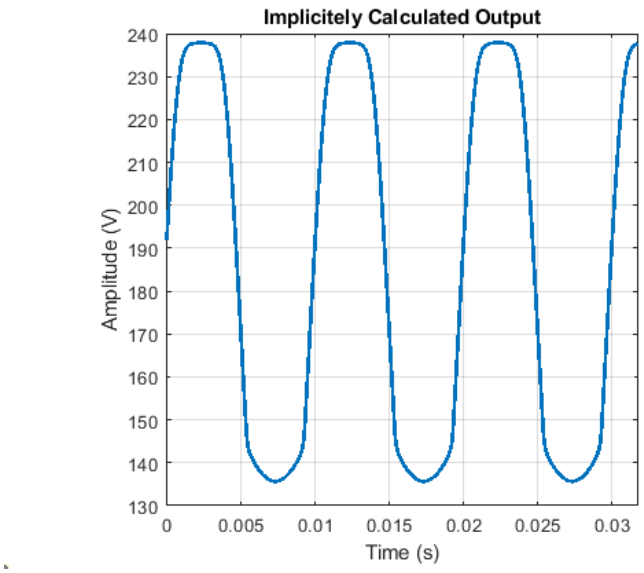

Figure 11: Simulation Output with Implicit Nonlinear Solver

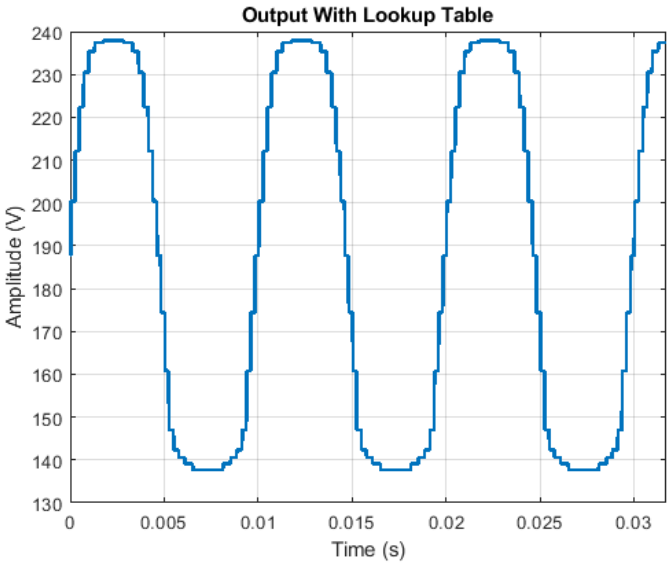

Figure 12: Simulation Output with Lookup Table

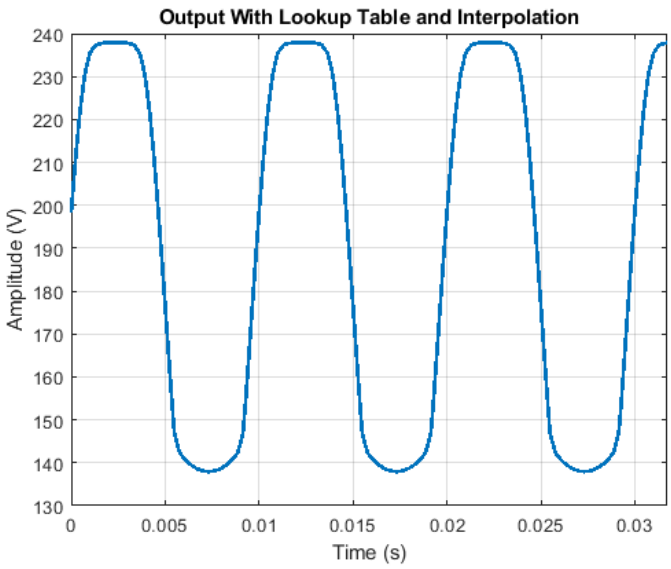

Figure 13: Simulation Output with Lookup Table and Bilinear Interpolation

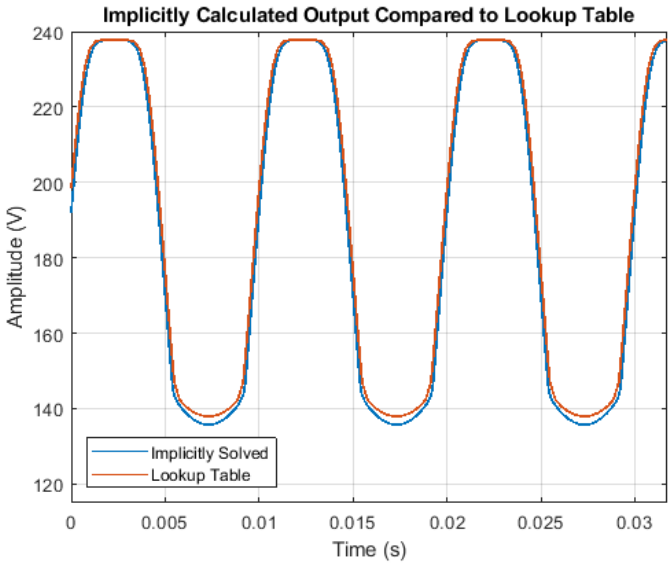

Figure 14: Comparison of Nonlinear Solver and Interpolated Lookup Table

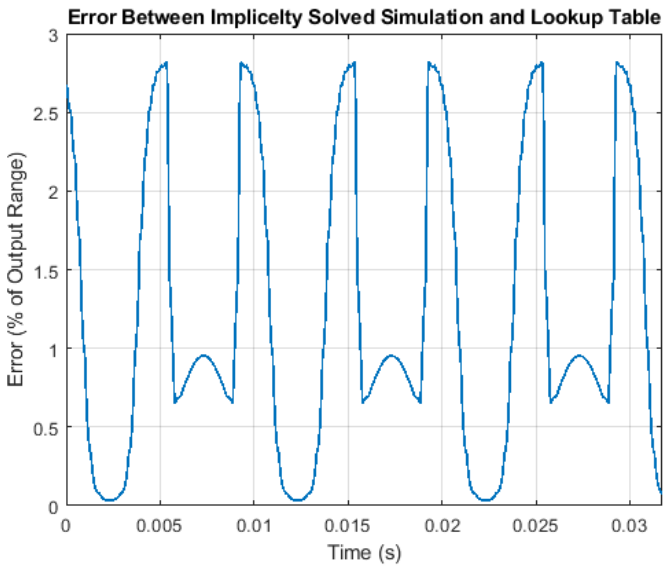

Figure 15: Error of Signals in Figure 11

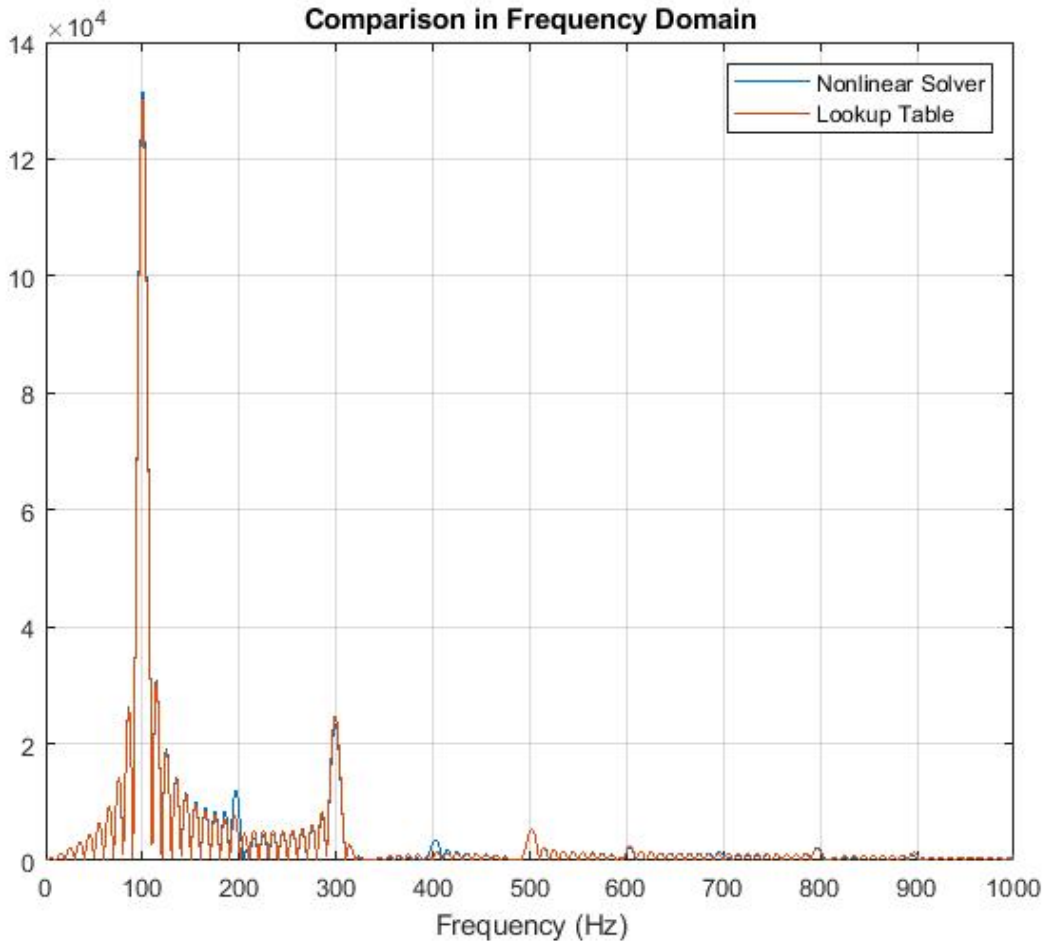

Figure 16: Comparison in the Frequency Domain

B. Algorithm to Model EQ System

To evaluate the effectiveness of the designed linear time invariant (LTI) digital filter used to simulate the tone stack frequency response, the digital filter response is compared to the s-domain response that is analytically derived from the schematic of the Fender Blues Jr. tonestack (Figure 6). Figure 17 shows the frequency response for different settings of the bass, middle, and treble knobs. Figure 18 shows the squared error vs frequency for all tone knobs set to one. Analytically deriving the digital filter from the circuit proved to be an extremely accurate method to simulate the tonestack system in real time.

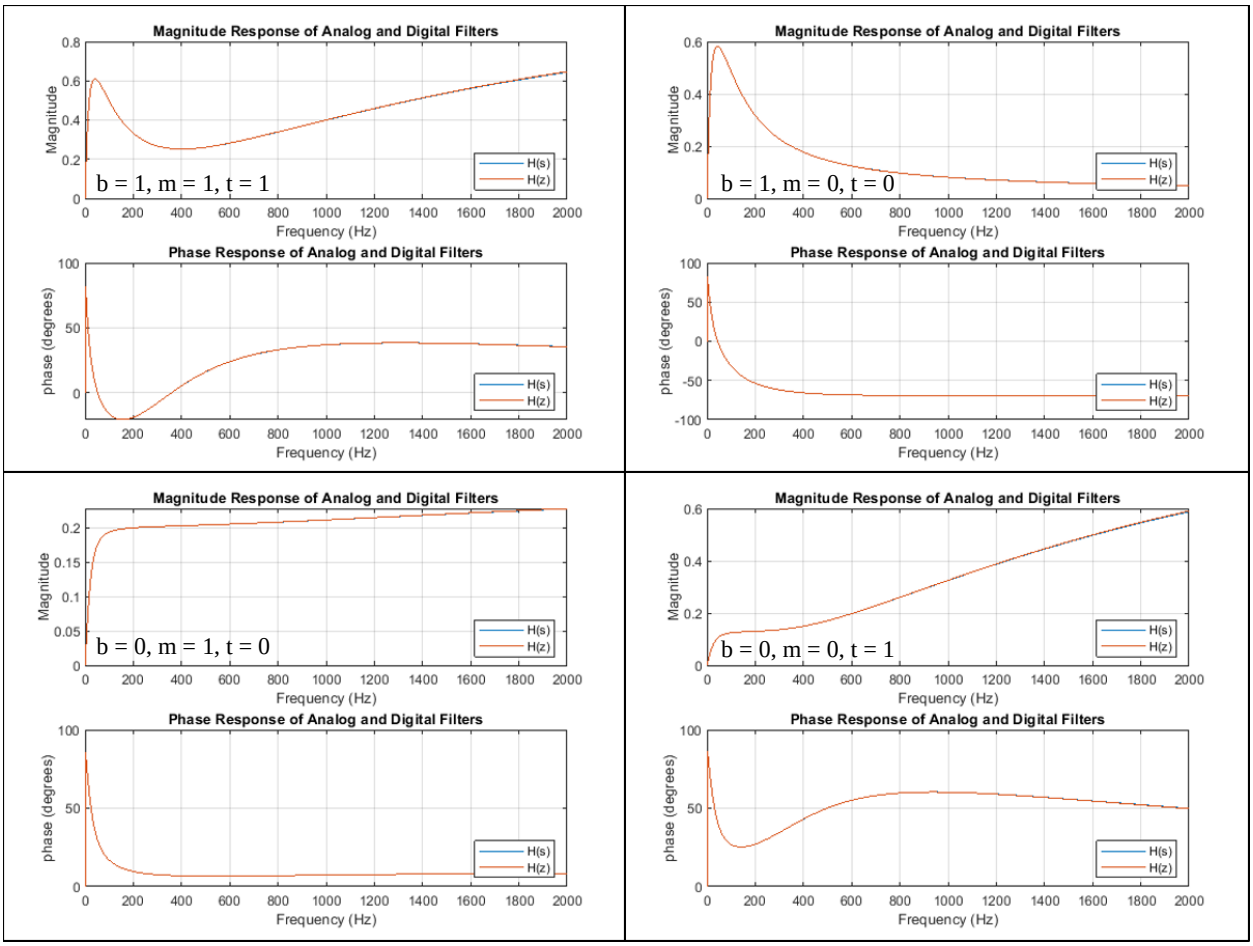

Figure 17: Frequency Response for various tone knob settings

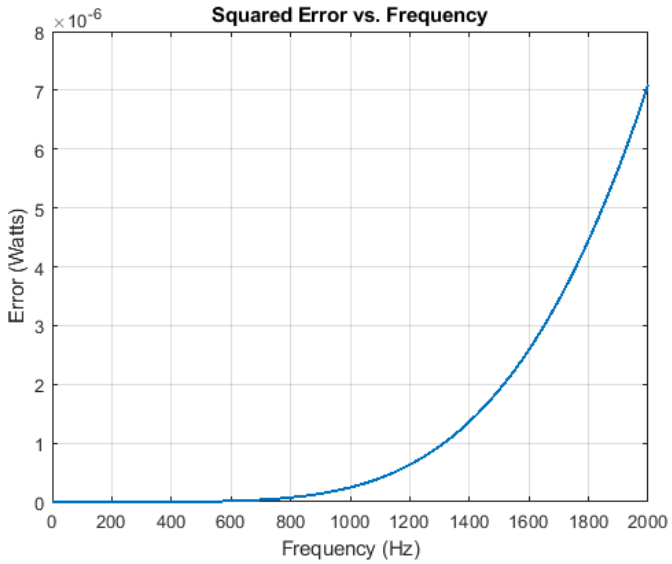

Figure 18: Squared Error vs. Frequency

C. Circuit Design

The audio output of the designed circuit had a very strong, unwanted sinusoidal noise. Looking at the signal path revealed that this noise was added after both low pass filter stages. Figure 19 shows the spectrum of the output without any input connected.

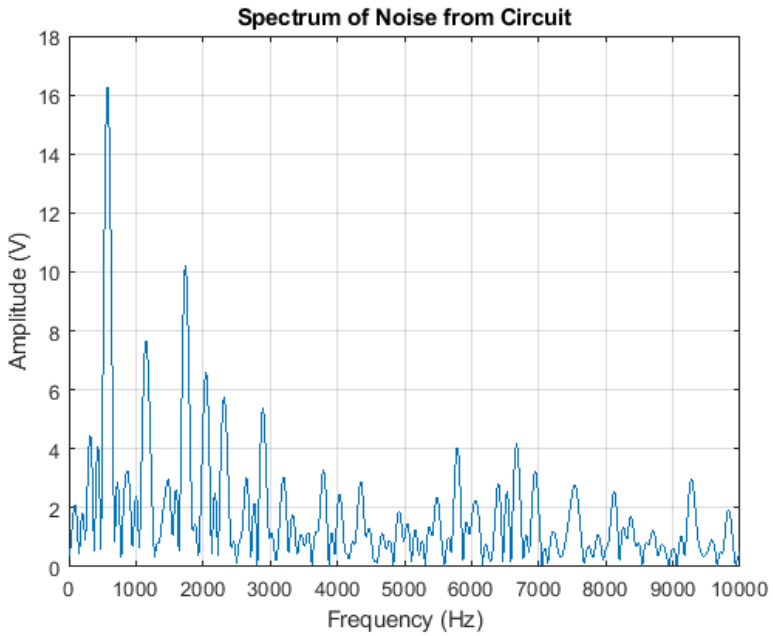

Figure 19: Discrete Fourier Transform of Noise from Circuit

In order to calculate the signal to noise ratio (SNR), the noise was measured by measuring the output with no input connected. The signal was assumed to be a sinusoid with the peak to peak value equivalent to the dynamic range of the output. This was measured to be 2.6 V. The signal to noise ratio of the circuit was calculated to be 26.33 dB. Since this digital artifact is not random, a post processing procedure was developed to eliminate some of the noise using digital filtering. The details of the designed digital filter are outlined in section VI.D.1. The SNR after post processing was calculated to be 30.57 dB.

In order to attempt to calculate the SNR as if the digital artifacts were not present, the SNR was calculated for bands in the frequency domain that avoided the digital noise. In order to

calculate this, Parseval's Thereom for the discrete instance (20) was used and the equation used for calculating the SNR is given in (21), where X_{signal} and X_{noise} are the discrete fourier transform of the measured signal and noise and l is in the range of chosen frequency bands shown in Figure 20.

$$\sum_{n=0}^{N-1}|x[n]|^2 = \frac{1}{N}\sum_{k=0}^{N-1}|X[k]|^2 \tag{20}$$

$$SNR = 10 \cdot \log\left(\frac{\sum_l \left|X_{signal}[k]\right|^2}{\sum_l |X_{noise}[k]|^2}\right) \tag{21}$$

Figure 20 shows a plot of the noise spectrum and the frequency bands that were chosen. The resulting SNR using this method was calculated to be 31.9 dB.

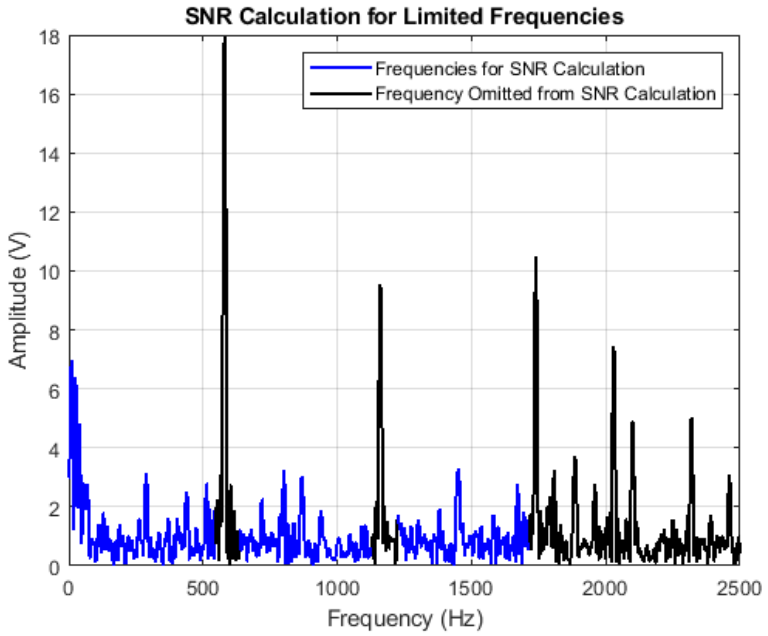

Figure 20: Bands used to calculate SNR without considering frequency spikes

D. Human Hearing Test

In order to evaluate how the Digital Guitar Amp audibly compared to the Fender Blues Jr, a human hearing survey was conducted. The form of the survey was a simple ABX test. This consists of playing the subject an audio recording of the output from the Digital Guitar Amp and the output of the Fender Blues Jr, while letting them know which audio they are listening to. Then, the subject is asked to identify the source of 10 randomly ordered audio samples. Lastly they are asked to comment on the differences that they heard in the two audio samples at the beginning.

1) Survey Setup and Experiment Design

Since the designed Digital Guitar Amp created a loud, unwanted digital noise the following method was used to evaluate the performance of the Digital Guitar Amp without consideration of the noise. The Fender Blues Jr. and the Digital Guitar Amp, plugged into a PA speaker, were set up side by side. Two, identical, microphones were pointed directly at each speaker cone respectively. The audio was then recorded for a single system, using both microphones in stereo while both systems were on. This resulted in the unwanted digital noise being present in both recordings. The audio was then imported into MATLAB and condensed into mono using (22).

$$X_{Mono} = \frac{1}{2}\left(X_{Left} + X_{Right}\right) \tag{22}$$

Since the digital noise was not random, as outlined in section VI.C, a digital notch filter was designed to cancel out most of the digital noise in post processing. 6 different notch filters were designed and implemented sequentially in MATLAB. The coefficients of these filters are given in Table 2. The noise cancelling MATLAB script and audio recordings used for the human

hearing survey are available at https://github.com/John-Ragland/Thesis.The values reported indicate a 9th order polynomial of the form given in (23).

$$H(z) = \frac{b(1) + b(2)z^{-1} + \cdots + b(n_b + 1)z_b^{-n_b}}{1 + a(2)z^{-1} + \cdots + a(n_a + 1)z^{-n_a}} \tag{23}$$

Table 1: Coefficients of Designed Noise Cancelling Filters

Filter 1		Filter 2		Filter 3		Filter 4		Filter 5	
a	b	a	b	a	b	a	b	a	b
1	0.972476	1	0.972463	1	0.972463	1	0.972463	1	0.972463
-7.92049	-7.75663	-7.73728	-7.57711	-7.85126	-7.68873	-7.5792	-7.4223	-7.58056	-7.42363
27.46987	27.0905	26.39408	26.02923	27.06039	26.68632	25.48611	25.13382	25.49382	25.14142
-54.4874	-54.1119	-51.8397	-51.4818	-53.4753	-53.1061	-49.6336	-49.2909	-49.6522	-49.3094
67.60642	67.61111	64.11077	64.11441	66.26828	66.272	61.21047	61.21399	61.23491	61.23843
-53.7319	-54.1119	-51.1209	-51.4818	-52.7338	-53.1061	-48.9454	-49.2909	-48.9638	-49.3094
26.71341	27.0905	25.66725	26.02923	26.31521	26.68632	24.78429	25.13382	24.79178	25.14142
-7.59559	-7.75663	-7.41989	-7.57711	-7.5292	-7.68873	-7.2683	-7.4223	-7.2696	-7.42363
0.945683	0.972476	0.945683	0.972463	0.945683	0.972463	0.945683	0.972463	0.945683	0.972463

2) Results from Human Hearing Survey

The human hearing survey was completed by 13 individuals of varying musical knowledge. When asked to self-rank their knowledge about guitar effects (where 0 was absolutely no knowledge and 10 is that you play guitar and have specific opinions about the tone of your guitar playing) the mean self-reported knowledge score was 5.46 with a standard deviation of 3.21. The participants were able to correctly label the source of the audio 59.23% of the time. The distribution of the accuracy is shown in Figure 21. If the Digital Guitar Amp was a perfect representation of the Fender Blues Jr, over enough samples, the ideal percentage would be 50%. These results indicate that the audible difference is at least nontrivial to distinguish. Further conclusions would require a larger sample size and a more carefully designed

experiment. The participants were also asked to comment on the difference that they heard in the first two clips, in which they were provided the source information.

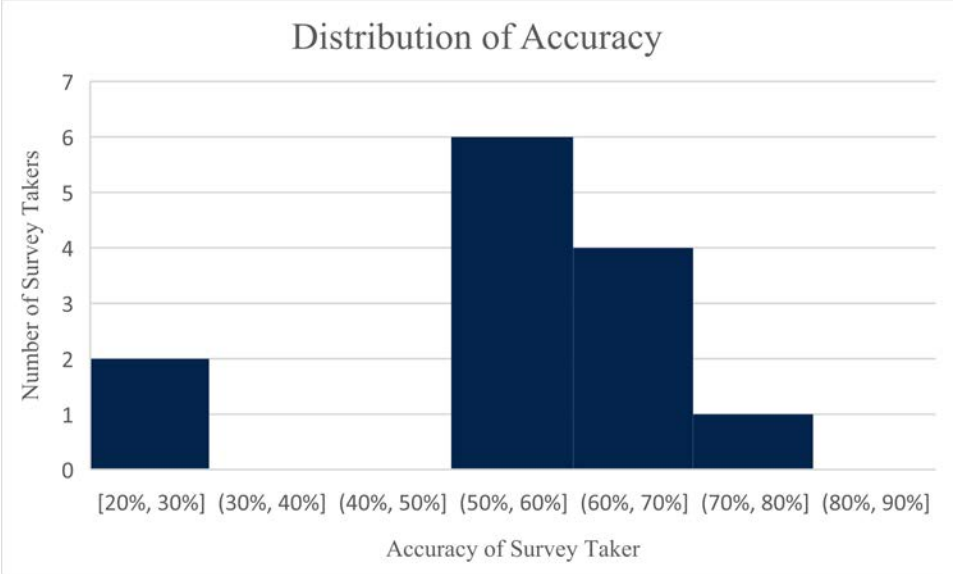

Figure 21: Distribution of Accuracy for the Human Hearing Survey

In order to investigate if some users took the test more seriously than others, the relationship between accuracy and the time the participant took on the test was observed. Figure 22 shows this relationship. The r^2 value was calculated to be 0.0021. There does not appear to be any correlation between how long the participant took on the survey and how well they performed.

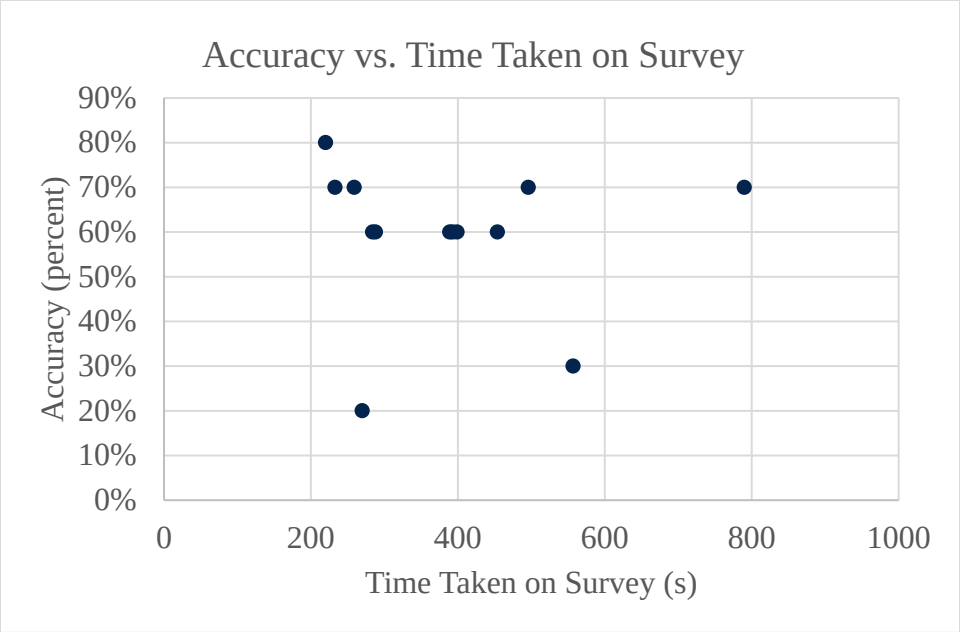

Figure 22: Plot of Accuracy versus Time

In order to investigate the effect of prior knowledge about guitar effects on the accuracy of the participants' guesses, a plot of accuracy vs self-reported guitar effect affluence is shown in Figure 23. The r^2 value for this data set was calculated to be 0.065, indicating no real significance.

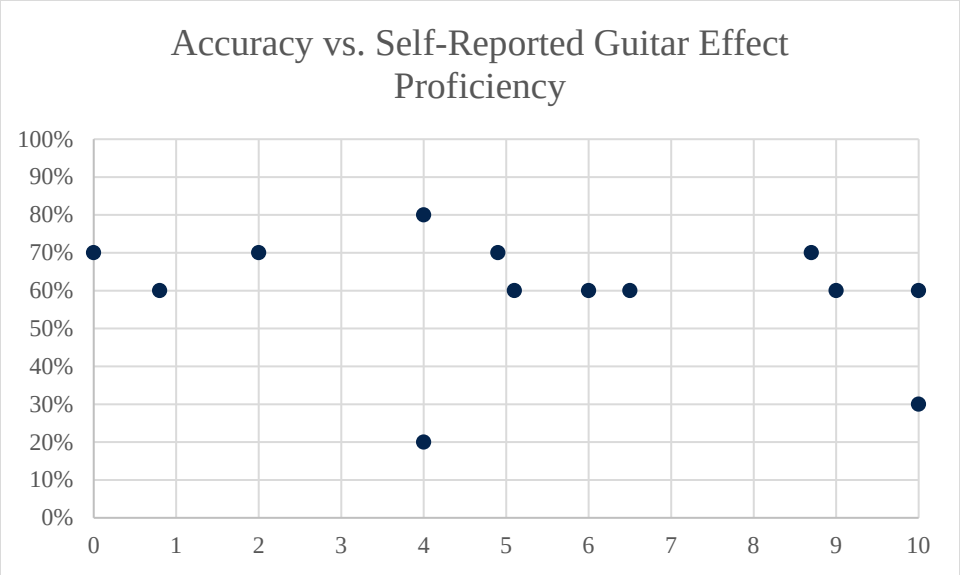

Figure 23: Plot of Accuracy versus Self Reported Guitar Effect Proficiency

A. Further Work

For the algorithm design, there were many areas that could be developed further. Namely, developing a real time simulation of the spring reverb and modeling the transformer characteristics. Further work to develop a circuit that does not contain the unwanted digital noise is also needed. Additionally, a true, peer reviewed human hearing test could better illuminate the differences between the real time physical model and the actual vacuum tube amplifier. There are a few recently published techniques that use machine learning to model a vacuum tube guitar amplifier. An analytical comparison of physical modelling techniques to the black box, machine learning techniques could aid in finding the best digital model for vacuum tubes. Lastly, the integration of all of this into a single guitar effects pedal could prove to be a viable product.

References

[1] R. O. Hamm, “Tubes Versus Transistors-Is There an Audible Difference,” *J. Audio Eng. Soc.*, vol. 21, no. 4, pp. 267–273, May 1973.

[2] B. Santo, “Volume cranked up in amp debate,” *Electron. Eng. Times*, no. 817, p. 4, Oct. 1994.

[3] T. Araya and A. Suyama, “SOUND EFFECTOR CAPABLE OF IMPARTING PLURAL SOUND EFFECTS LIKE DISTORTION AND OTHER EFFECTS,” 5570424.

[4] M. Doidic, M. Mecca, M. Ryle, and C. Senffner, “Tube modeling programmable digital guitar amplification system,” US5789689A, Aug. 04, 1998.

[5] S. Toyama, “Harmonic tone generator for low level input audio signals and small amplitude input audio signals,” US5578948A, Nov. 26, 1996.

[6] R. Kuroki and T. Ito, “DIGITAL AUDIO SIGNAL PROCESSOR WITH HARMONICS MODIFICATION,” 5841875, 1998.

[7] D. T. Yeh, J. S. Abel, and J. O. Smith, “Automated Physical Modeling of Nonlinear Audio Circuits For Real-Time Audio Effects—Part I: Theoretical Development,” *IEEE Trans. Audio Speech Lang. Process.*, vol. 18, no. 4, pp. 728–737, Oct. 2009, doi: 10.1109/TASL.2009.2033978.

[8] D. T. Yeh, “Automated Physical Modeling of Nonlinear Audio Circuits for Real-Time Audio Effects—Part II: BJT and Vacuum Tube Examples,” *IEEE Trans. Audio Speech Lang. Process.*, vol. 20, no. 4, pp. 1207–1216, May 2012, doi: 10.1109/TASL.2011.2173677.

[9] “Service Diagram, Combined (PCB assy) Blues Junior Rev. D.” [Online]. Available: https://www.thetubestore.com/lib/thetubestore/schematics/Fender/Fender-Blues-Junior-III-Schematic-Rev-D.pdf.

[10] H. Laurens, “Electrical musical instrument,” US2230836A, Feb. 04, 1941.

[11]N. Koren, “Improved vacuum tube models for SPICE simulations,” *Glass Audio*, vol. 8, no. 5, p. 18, 1996.

[12]J. C. Butcher, *Numerical Methods for Ordinary Differential Equations*. John Wiley & Sons, 2004.

[13]G. A. Shultz, R. B. Schnabel, and R. H. Byrd, “A Family of Trust-Region-Based Algorithms for Unconstrained Minimization with Strong Global Convergence Properties,” *SIAM J. Numer. Anal.*, vol. 22, no. 1, pp. 47–67, Feb. 1985, doi: 10.1137/0722003.

[14]D. T. Yeh and J. O. Smith, “Discretization of the ’59 Fender Bassman Tone Stack,” p. 5, 2006.

[15]“Teensy 4.0 - PJRC Store.” https://www.pjrc.com/store/teensy40.html (accessed Feb. 25, 2020).

[16]“opa2313-q1.pdf.” Accessed: Apr. 08, 2020. [Online]. Available: http://www.ti.com/lit/ds/symlink/opa2313-q1.pdf?HQS=TI-null-null-mousermode-df-pf-null-wwe&DCM=yes&ref_url=https%3A%2F%2Fwww.mouser.com%2F&distId=26.

[17]“LTC1069-6 - Single Supply, Very Low Power, Elliptic Lowpass Filter.” Linear Technology.

[18]“MAX11100 16-Bit, +5V, 200ksps ADC with 10uA Shutdown.” Maxim Integrated.

[19]“MAX6029 Ultra-Low-Power Precision Series Voltage Reference.” Maxim Integrated, [Online]. Available: https://datasheets.maximintegrated.com/en/ds/MAX6029.pdf.

[20]“LTC1655 16-Bit Rail-to-Rail Micropower DACs in SO-8 Package.” Linear Technology, [Online]. Available: https://www.mouser.com/datasheet/2/609/16555lf-1268941.pdfx.

Appendix I.

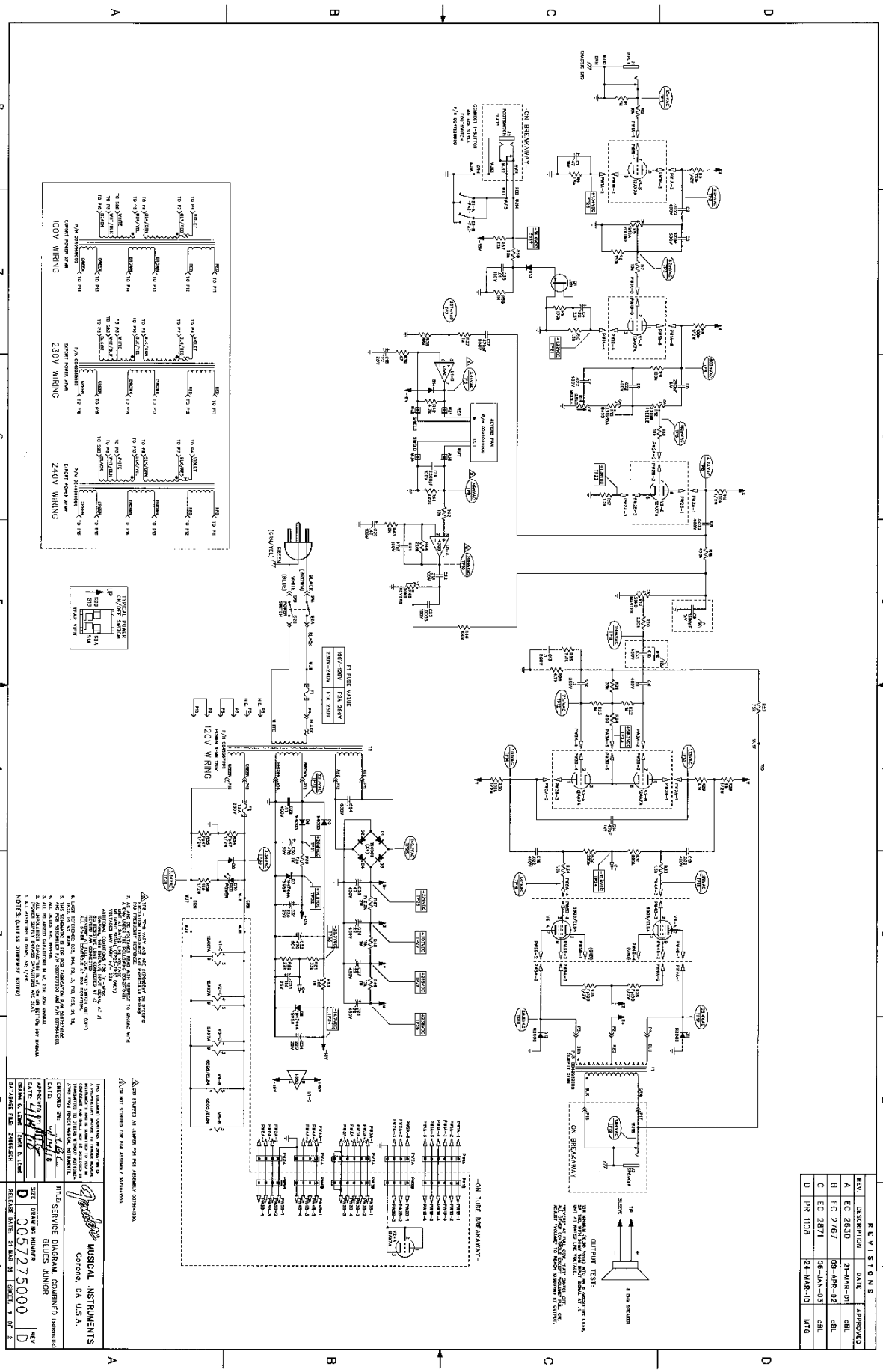
REVISIONS
REV | DESCRIPTION | DATE | APPROVED
A | EC 2830 | 21-MAR-01 | dBL
B | EC 2767 | 09-APR-02 | dBL
C | EC 2871 | 06-JAN-03 | dBL
D | PR 1108 | 24-MAR-10 | MTG
MUSICAL INSTRUMENTS
Corona, CA U.S.A.
TITLE SERVICE DIAGRAM, COMBINED (schematic)
BLUES JUNIOR
DRAWING NUMBER
005727500
SIZE D
REV D
RELEASE DATE 21-MAR-01
SHEET 1 OF 2
100V WIRING
230V WIRING
240V WIRING
120V WIRING
-ON BREAKAWAY-
-ON TUBE BREAKAWAY-
OUTPUT TEST
8 OHM SPEAKER

Appendix II.

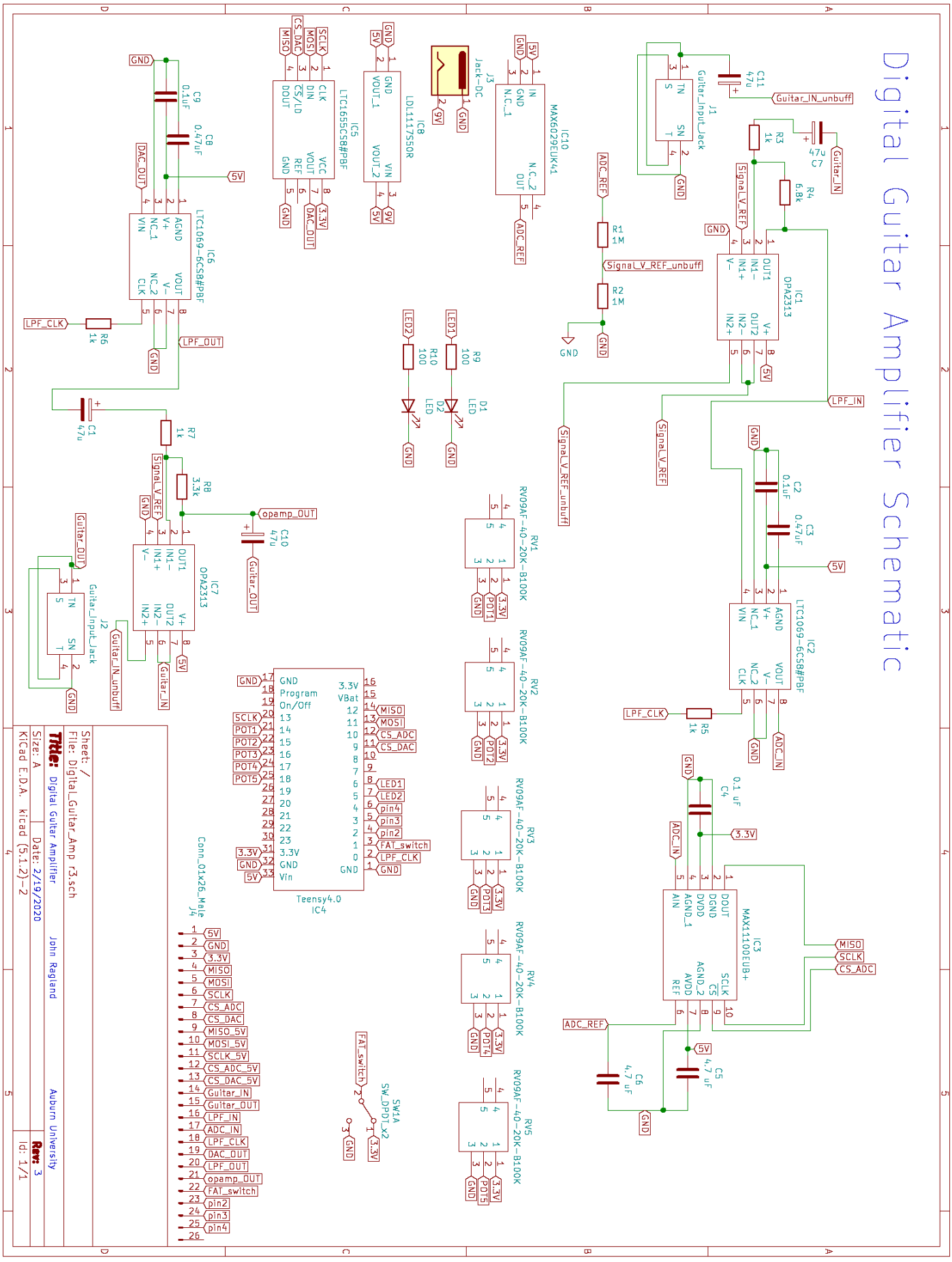
Digital Guitar Amplifier Schematic
Sheet: /
File: Digital_Guitar_Amp_r3.sch
Title: Digital Guitar Amplifier
John Ragland
Auburn University
Size: A
Date: 2/19/2020
Rev: 3
KiCad E.D.A. kicad (5.1.2)-2
Id: 1/1
Guitar_IN_unbuff
Guitar_IN
Guitar_Input_Jack
J1
C11 47u
R3 1k
R4 6.8k
Signal_V_REF
ADC_REF
R1 1M
R2 1M
Signal_V_REF_unbuff
IC1 OPA2313
LPF_IN
Signal_V_REF
Signal_V_REF_unbuff
C2 0.1uF
C3 0.47uF
IC2 LTC1069-6CS8#PBF
LPF_CLK
R5 1k
ADC_IN
C4 0.1 uF
IC3 MAX1100EUB+
MISO
SCLK
CS_ADC
C5 4.7 uF
C6 4.7 uF
IC10 MAX6029EUK41
J3 Jack-DC
IC8 LDL1117S50R
IC5 LTC1655CS8#PBF
C9 0.1uF
C8 0.47uF
DAC_OUT
IC6 LTC1069-6CS8#PBF
LPF_CLK
R6 1k
LPF_OUT
C1 47u
R7 1k
R8 3.3k
opamp_OUT
C10 47u
Guitar_OUT
IC7 OPA2313
J2 Guitar_Input_Jack
Guitar_IN_unbuff
LED1
LED2
R9 100
R10 100
D1 LED
D2 LED
RV1 RV09AF-40-20K-B100K
RV2 RV09AF-40-20K-B100K
RV3 RV09AF-40-20K-B100K
RV4 RV09AF-40-20K-B100K
RV5 RV09AF-40-20K-B100K
POT1
POT2
POT3
POT4
POT5
IC4 Teensy4.0
Program On/Off
3.3V VBat
MISO
MOSI
CS_ADC
CS_DAC
LED1
LED2
pin4
pin3
pin2
FAT_switch
LPF_CLK
J4 Conn_01x26_Male
SW1A SW_DPDT_x2
FAT_switch